

# Review of Trees Using Medical Radiological Equipment

**Damir Ciprić<sup>1</sup>, Velimir Karadža<sup>1</sup>, Vladimir Kušan<sup>2</sup>, Frane Mihanović<sup>3</sup>, Branko Kovalisko<sup>4</sup>**

<sup>1</sup> University of Applied Health Sciences, Zagreb, Croatia

<sup>2</sup> OIKON d.o.o., Institute for Applied Ecology, Zagreb, Croatia

<sup>3</sup> University of Split, Faculty of Health Sciences, Split, Croatia

<sup>4</sup> "Dr. Juraj Njavro" National Memorial Hospital, Vukovar, Croatia

**Corresponding author:** Damir Ciprić, email: [damir.cipric@gmail.com](mailto:damir.cipric@gmail.com)

**DOI:** [10.55378/rv.49.2.2](https://doi.org/10.55378/rv.49.2.2)

## Abstract

In continental lowland forests, an increase in the poor health status of ash trees has been observed in recent years. This study investigated the capabilities of modern radiological equipment for the cross-sectional imaging of tree trunks, specifically to determine whether a medical radiological device can visualize ash tree disease. Since a comparison of the performed radiological tomographic scans and existing photographs of the same samples showed that the changes visible on the photographs could also be seen on the radiographic images, the aim of this research was achieved. This confirms that the use of appropriate radiological equipment is satisfactory for the detection of changes caused by infectious diseases or other issues in ash trees.

**Keywords:** radiography, non-invasive scanning, structural wood imaging, pathogenic change detection, ionizing radiation

## Introduction

Analyses of the common ash tree, its crown, trunk, root system, and surrounding soil in the forests of Posavina (Croatia) have confirmed the presence of multiple species of fungi and similar organisms that inhabit trees of varying health status. The frequency of certain pathogenic species, particularly *Hymenoscyphus fraxineus*, species from the genus *Armillaria*, and *Lentinus tigrinus*, increases with a deteriorating health status. It was found that pathogens occur almost equally across all common ash forests [1].

Ash tree diseases, especially when occurring epidemically, significantly reduce the industrial value of the wood. Early detection is crucial to preserve the material value of the timber. Although the rise of "poor health" in ash trees can be attributed to various diseases, this study investigates the possibility of "in vivo" detection to industrially utilize those trees where the infection is in its initial phase. While the quality of wood surfaces is easily observable, structural characteristics and internal defects in the wood are difficult to ascertain solely from external appearance. The conventional method for observing internal wood structure is cutting down the tree. However, non-invasive testing technologies such as stress wave, ultrasound, or 2D/3D medical radiological devices provide the ability to select which trees should be felled. This feature – the non-destructive evaluation of the interior of logs using ionizing radiation – allows for detailed visualization of internal struc-

tures: knots, porosity, growth rings, cracks, pests, and diseases. This enables the determination of applicability in the timber industry, construction (for testing the quality

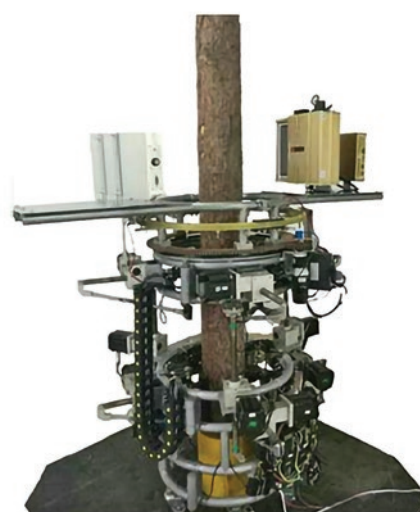


**Figure 1:** Illustration of a test system for non-invasive scanning of living trees

Source: Ge, Z. D., Hou, X. P., Li, Z. F., and Zhou, Y. C. "Application of computed tomography (CT) in non-destructive testing of wood



**Figure 2.** Photograph of a trunk cross-section with visible changes



**Figure 3.** Photograph of a trunk cross-section of a second sample without visible changes

of recycled wood), and the restoration of valuable wooden objects [2, 3].

In the early 1990s, medical CT (Computed Tomography) devices were used to image the internal structural characteristics of wood and wooden building materials [4, 5]. However, CT scanners are medical devices primarily used for radiology diagnostics and are not suitable for scanning fixed and immovable objects, such as living trees or timber-framed buildings. To utilize CT technology in such situations, layered scanning platforms for these objects have been developed [6].

Although ionizing radiation has been used in forestry and the timber industry since the late 1980s for research and later as an industrial tool, we investigated whether modern medical radiological devices, particularly technology with continuously improving image receptors, more mobile designs, and modern software solutions for image

processing, could provide the same or better structural wood images than previous research.

The aim was to visualize ash wood damage on a CT scan, which was also visually apparent in a cross-section of the trunk (Figure 2), and to check whether changes could be detected by measuring density even if they were not visually noticeable on another cross-section (Figure 3).

## Materials and Methods

### Sample Acquisition

The initial phase of the research utilized a multi-slice CT device with 16 detector rows at the lowest possible exposure settings.

A total of ten transverse ash trunk cross-sections (disks), approximately thick, were received from two areas



**Figure 4:** C-arm

Source: <https://www.ziehm.com>



(Lonja and Radinje). This was deemed sufficient for initial investigation, with samples showing varying degrees of structural change.

### Image Acquisition

All samples were initially scanned on the device under identical conditions (80 kV and 190 mA) to ensure the energy of the ionizing radiation was similar to that of mobile devices.

In a later phase, all samples were re-scanned using a radiological C-arm capable of Cone Beam CT imaging (CBCT). This device is relatively light and suitable for field use. The C-arm utilized a cone-beam principle, capturing an image after slightly more than half rotation (180 degrees) of the X-ray tube and detector around the object.

### Data Analysis and Measurement

On the image records, density measurements were taken in Regions of Interest (ROI) that showed visible changes, areas that visually appeared suspicious, and areas that were clearly healthy.

Since C-arm devices provide the image record in a "gray scale" rather than in Hounsfield Units (HU), density measurements could not be performed directly. However, future possibilities exist to achieve this using the same devices with appropriate software programs [7].

For the analysis of changes, the relative density of the (zone/volume of interest) was measured on all samples and compared with the density of the healthy wood tissue volume.

The scans were also processed in viewing software, where contrast and windowing were adjusted to highlight

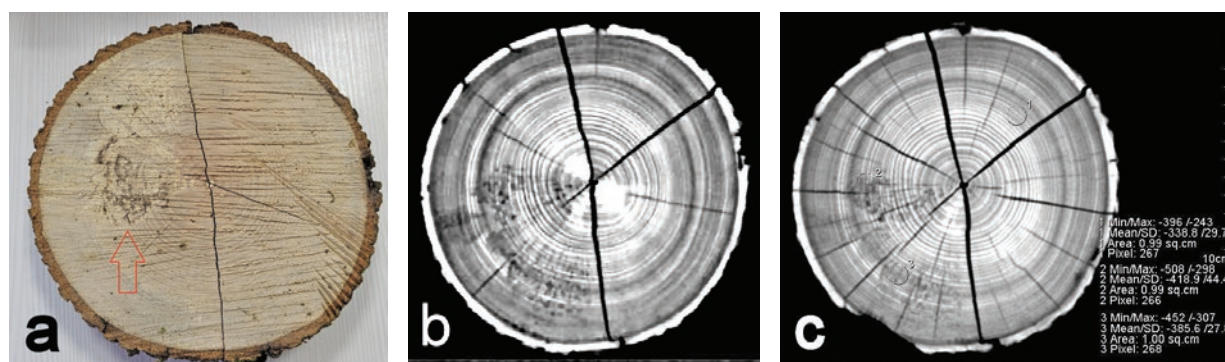


**Figure 5.** Sample Lonja 2, a) photograph, b) CT scan, c) CT scan with ROI values

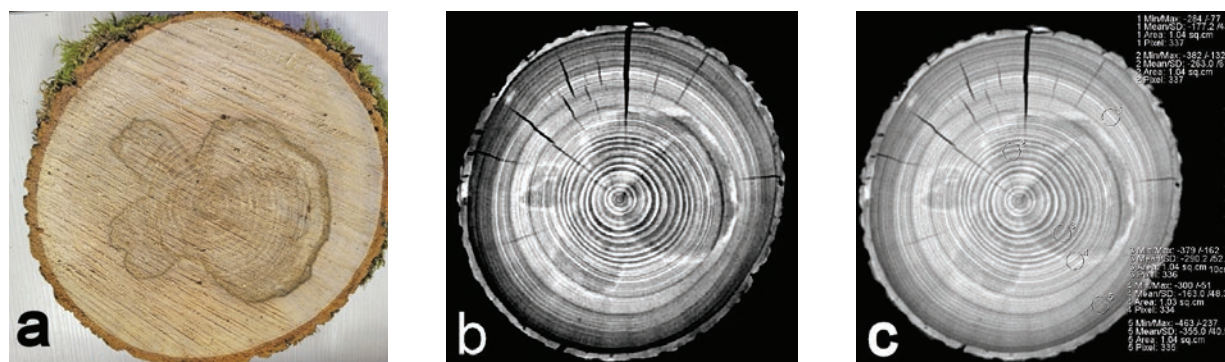


**Figure 6.** Sample Lonja 4, a) photograph, b) CT scan, c) CT scan with ROI values

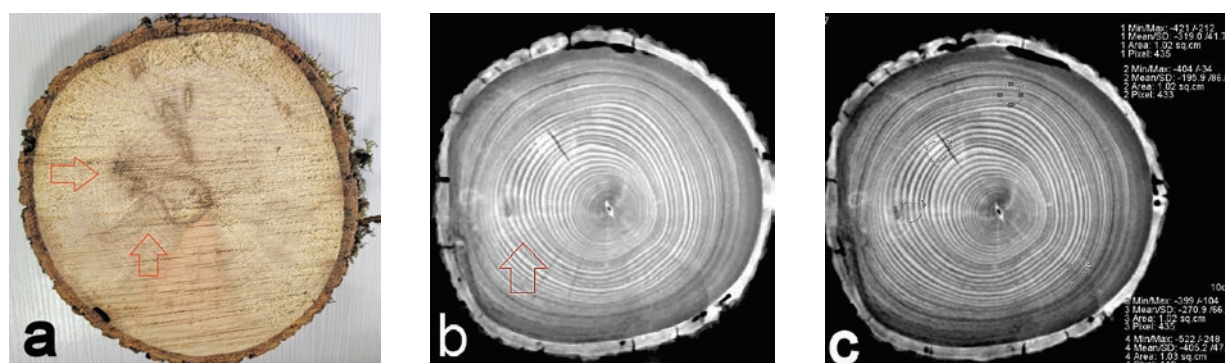


**Figure 7.** Sample Radinje 1, a) photograph, b) CT scan, c) CT scan with ROI values

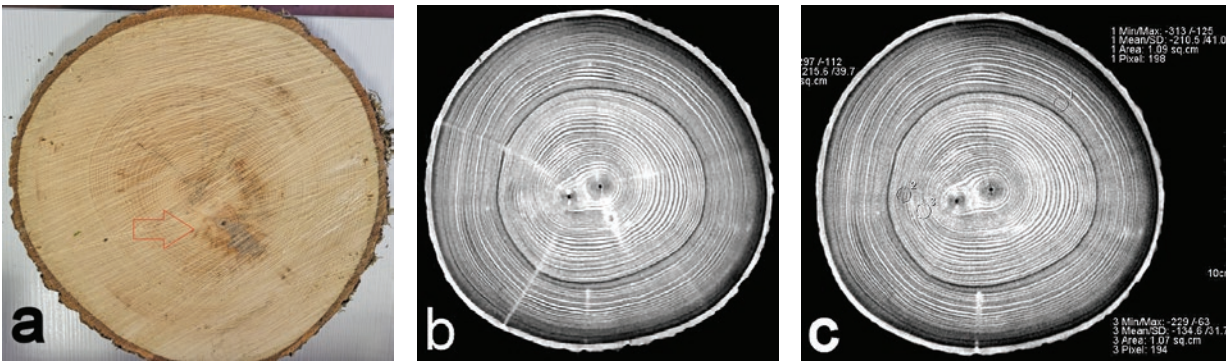


Figure 8. Sample Radinje 5, a) photograph, b) CT scan, c) CT scan with ROI values

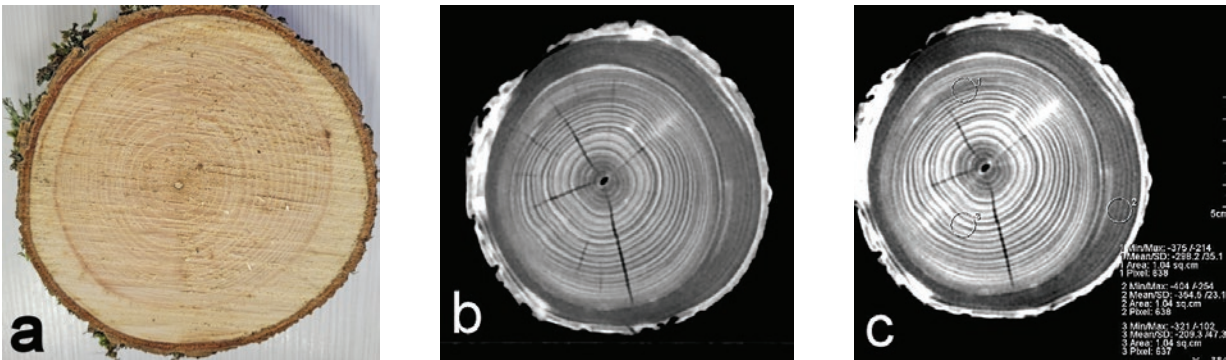


Figure 9. Sample Lonja 1, a) photograph, b) CT scan, c) CT scan with ROI values

the changes, making them more easily observable (Figures 5 to 9).

Figures 5-9 illustrate comparative photographs, CT cross-sections, and cross-sections with values for various samples (Lonja 2, Lonja 4, Rad 1, Rad 5, Lonja 1).

For a quantitative evaluation, the mean density values (HU) within the ROIs were collected and organized into tables for samples from both the Lonja and Radinje areas.

Results

Qualitative Results (Visual Confirmation)

Visual comparison of and scans with photographs of the same samples showed that changes visible on the photographs could also be clearly observed on the radiological images (C-arm – e.g., Figures 10 and 11).

Although the images were of lower quality (due to lower exposure values and possible poor positioning), they still displayed visible changes in the sample’s condition, similar to the scans.

Quantitative Results (HU Measurement)

Tables 1 and 2 present the results of relative density measurements for the ROI in the samples from the Lonja and Radinje areas, respectively.

Table 1. Measurement of Relative Density for Lonja Samples

Sample	Category	MIN / MAX	Mean /SD	cm <sup>2</sup>	Pixels
Lonja 1	damaged	-375/-214	-298,2/35,1	1,04	638
	suspect	-404/-254	-354,5/23,1	1,04	638
	healthy	-321/-102	-209,3/47,3	1,04	637
Lonja 2	damaged	-508/-298	-418/44,4	0,99	266
	suspect	-452/-307	-385,6/27,8	1,00	268
	healthy	-396/-243	-338,8/29,7	0,99	267
Lonja 3a	damaged	-425/-195	-301,6/38,5	1,01	336
	suspect	-446/-267	-373,5/39,5	1,01	335
	healthy	-345/-208	-271,6/26,6	1,01	335
Lonja 3	damaged	-441/-208	-328,4/51,1	1,01	336
	suspect	-435/-251	-372,5/25,3	1,01	336
	healthy	-338/-232	-279,9/20,6	1,01	335
Lonja 4	damaged	-379/-162	-290,2/52,8	1,04	336
	suspect	-382/-132	-263/61	1,04	337
	healthy	-284/-77	-177/43	1,04	337



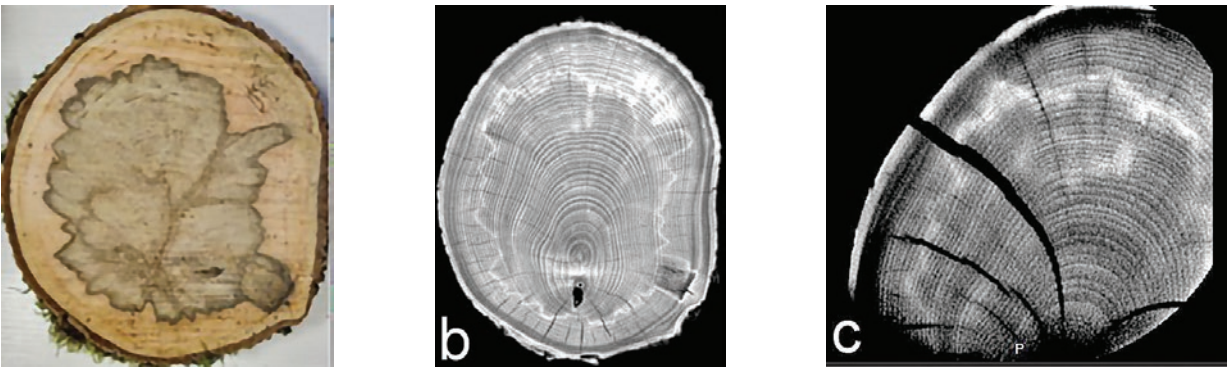


**Figure 10.** Sample Lonja 3, a) photograph, b) CT scan, c) cross-section with C-arm source

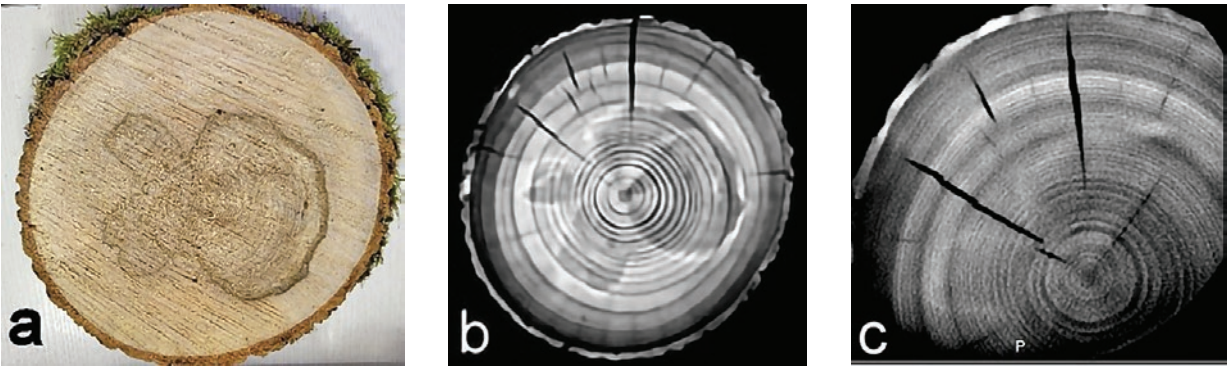


**Figure 11.** Sample Lonja 4, a) photograph, b) CT cross-section, c) cross-section with C-arm source

**Table 2.** Measurement of Relative Density for Radinje Samples

Sample	Category	MIN / MAX	Mean /SD	cm <sup>2</sup>	Pixels
R 1	damaged	-522/-248	-405/47,8	1,03	440
	suspect	-404/-34	-196/86,8	1,02	433
	healthy	-421/-212	-319/41,7	1,02	435
R 22	damaged	-272/3	-115,4/57,5	1,12	163
	suspect	-312/-80	-200/50,2	1,16	168
	healthy	-390/-230	-328,7/26,4	1,07	156
R 3	damaged	-135/34	-39,9/35,	1,08	196
	suspect	-227/72	-85,5/57	1,05	190
	healthy	-401/-260	-338/28,2	1,10	200
R 4	damaged	-300/-61	-183,3/56,2	1,09	125
	suspect	-352/-214	-291,3/26	1,09	125
	healthy	-374/-235	301,8/3,4	1,09	125
R 5	damaged	-229/-63	-134,6/31,7	1,07	194
	suspect	-297/-112	-215,6/3,7	1,05	191
	healthy	-313/-125	-210/41	1,09	198
R 66	damaged	-525/-348	-444,3/38,8	1,13	70
	suspect	-369/-237	-313,1/30,6	1,05	65
	healthy	-448/-324	-394,6/26,4	1,10	68

The measured mean densities for damaged and suspect areas consistently showed a lower value (lower density) compared to the healthy section of the sample. The difference between HU is roughly equivalent to a difference in wood mass, suggesting that visible changes correspond to a reduction in wood mass. Relatively higher density values in samples R3 and R4 (with some positive values) are likely a consequence of the freshness of those samples.

From the numerical and especially from the graphical representation, an equal difference is visible between the minimum (MIN), average (MEAN) and maximum (MAX) wood density: chart 1. for samples from the Lonja area and chart 2. for samples from the Radinje area.

The areas were of approximately the same surface area, but the number of pixels varied significantly due to the use of different magnifications.

To confirm the usability of mobile radiological equipment, all samples were scanned with two C-arm devices from the same manufacturer. Although the scans were performed with lower exposure values and suffered from deformed or partial images due to inexperience with this application, the resulting images still displayed the visible changes in the samples, similar to the CT scans (Figures 10 and 11).

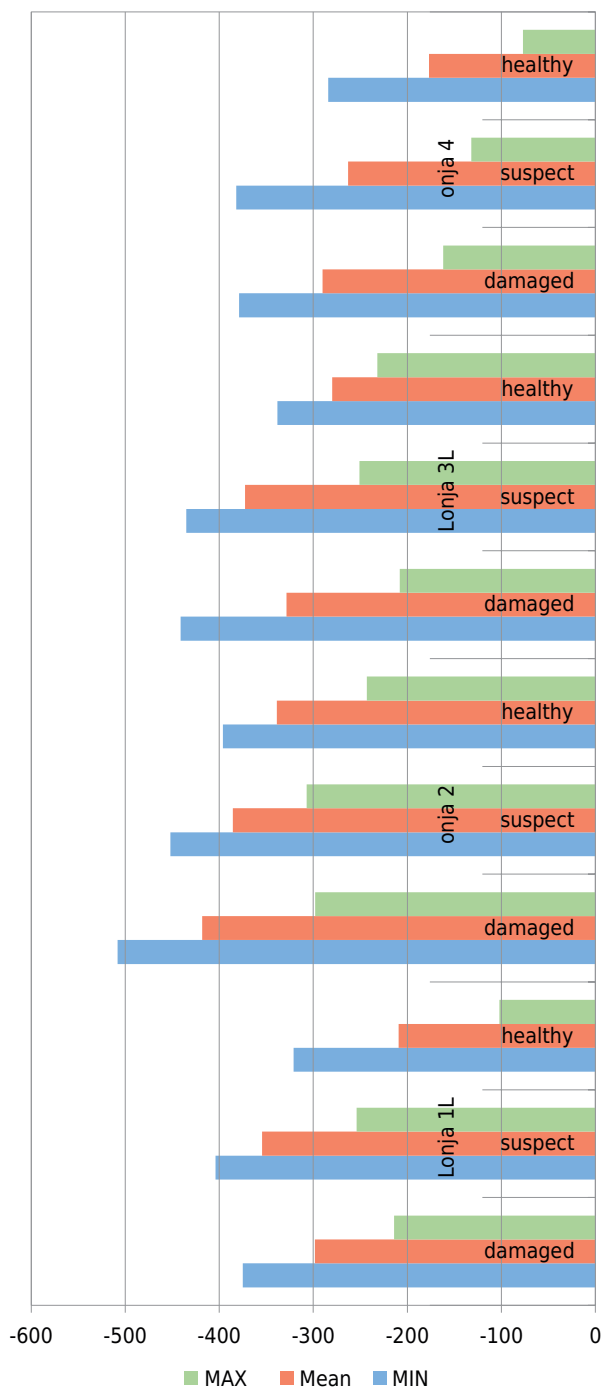


**Chart 1.** showing sample density from the Lonja area

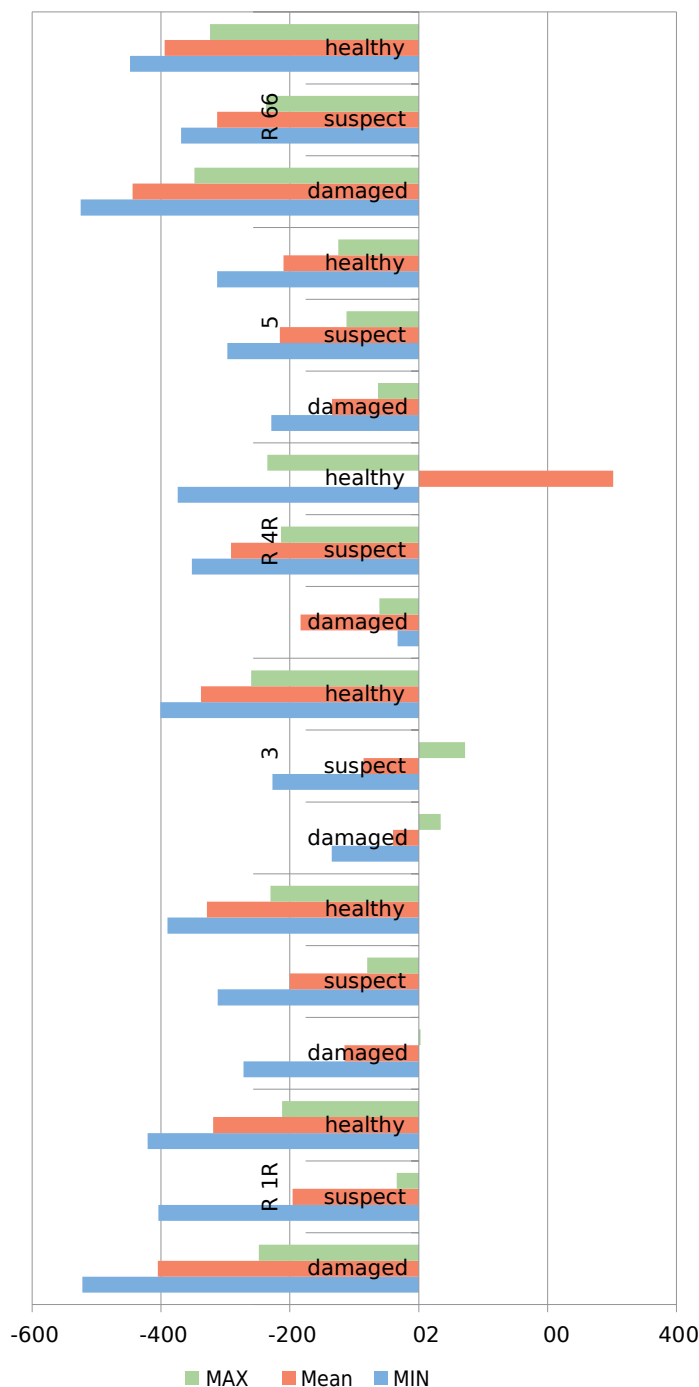


**Chart 2,** showing sample density from the Radinje area

## Discussion

The variation in the number of pixels for approximately the same surface area is a result of using different magnifications to achieve a comparable cross-sectional image of trunks with different diameters. A larger number of pixels for a given area, or a smaller pixel size, increases spatial resolution. This provides a more detailed display, and placed on a smaller, specific structure will more accurately reflect the true attenuation values of that structure. Conversely, when pixels are too large, they may average the values of multiple different materials within the field,

leading to a less accurate value [8]. Reducing the pixel size also decreases the number of photons detected per pixel, which can increase the image noise level and introduce inconsistency in measurements [9]. Nevertheless, in this case, the mean values can still be reliably used for evaluation and comparison.

The mean density values for visible changes presented in the tables show a lower intensity in values (i.e., lower density) in the damaged samples compared to the healthy sections. This reduction in density (estimated at 10 to 20 % of wood mass) suggests lower quality timber but does not allow for precise determination of the type or cause of the change.

## Conclusion

From the collected image records obtained from different devices, structural changes in the ash trunk cross-section are clearly observable and correspond to the colour changes visible in the photographs of the same samples, despite the varying quality of the images. When using imaging that provides density values (HU), the density is quantifiable, ensuring a more accurate detection of changes in wood quality.

The utility of modern radiological equipment for cross-sectional visualization of tree trunks is confirmed by the presented examples. Since the comparison of CT and CBCT scans with photographs of the same samples showed that the visible changes can be observed on the radiological image, we conclude that the research goal has been achieved: the use of appropriate radiological equipment is sufficient for the detection of damage in infected ash trees.

## Pregled stabala medicinskom radiološkom opremom

### Sažetak

U kontinentalnim nizinskim šumama, zadnjih je godina zapažen porast lošeg zdravstvenog stanja stabala jasena. U ovom radu su istražene mogućnosti suvremene radiološke opreme u slikovnom prikazu presjeka debla, odnosno može li se medicinskim radiološkim uređajem vizualizirati bolest stabla jasena. Kako je usporedba učinjenih radioloških tomografskih snimaka i već postojećih fotografija istih uzoraka pokazala da se promjene na fotografijama mogu vidjeti i na radiografskom zapisu, cilj ovog istraživanja je ostvaren u dijelu da je potvrđeno kako uporaba odgovarajuće radiološke opreme zadovoljava u detekciji promjena uzrokovane zaraznim bolestima stabala jasena ili drugim uzrocima.

**KLjučne riječi:** radiografija, neinvazivno skeniranje, strukturno snimanje drva, otkrivanje patogenih promjena, ionizirajuće zračenje

### Literature:

1. D. Diminić, J. Kranjčec Orlović, Bolesti poljskog Jasena, Poljski jase u Hrvatskoj, Akademija šumarskih znanosti, CIP 001139257, ISBN 978-953-98571-7-0, Zagreb 2022.
2. A. Uldry, B. P. Husted, I. Pope, L. M. Ottosen: A Review of the Applicability of Non-destructive Testing for the Determination of the Fire Performance of Reused Structural Timber, Open access, Published: 21 September 2024, Volume 43, article number 106, (2024)
3. P. WITOMSKI, A. KRAJEWSKI, T. NAROJEK, Measurements of wood density using X-ray computer tomography, Faculty of Wood Technology, Warsaw University of Life Sciences – SGGW (WULS-SGGW)
4. Jacobs, P., Sevens, E., and Kunnen, M. (1995). "Principles of computerized X-ray tomography and applications to building materials," *The Science of the Total Environment* 167(1-3), 161-170.
5. Livingston, R. A. (1999). "Nondestructive testing of historic structures," *Archives and Museum Informatics* 13(3-4), 249-271.
6. Ge, Z. D., Hou, X. P., Li, Z. F., and Zhou, Y. C. (2016). "Application of computed tomography (CT) in nondestructive testing of wood," *China Wood Industry* 30(3), 49-52.
7. Kovalisko, B. (2024), „Validacija sive skale na C-Luku u korelaciji s HU na CT-u“ (Diplomski rad). Split: Sveučilište u Splitu. Available at: <https://urn.nsk.hr/urn:nbn:hr:176:250840>
8. C. E. Carter, B. L. Vealé, „*Digital Radiography and PACS*“, Book ISBN: 978-0-323547581,
9. Mackin D, Fave X, Zhang L, Yang J, Jones AK, Ng CS, and others, Harmonizing the pixel size in retrospective computed tomography radiomics studies, *PLoS One*. 2018 Jan 17;13(1): e0191597. eCollection 2018, PMID: 29342209.